THE AMERICAN SOCIETY OF MECHANICAL ENGINEERS
345 E. 47 St., New York, N.Y. 10017

89-GT-272

Heat Transfer in Rotating Passages with Smooth Walls and Radial Outward Flow

J. H. WAGNER
B. V. JOHNSON
United Technologies
Research Center
East Hartford, CT

T. J. HAJEK
Commercial Engine Business
Pratt and Whitney Division
East Hartford, CT

ABSTRACT

Experiments were conducted to determine the effects of rotation on heat transfer in turbine blade internal coolant passages. The experiments were conducted with a smooth wall, large scale heat transfer model. The objective was to obtain the heat transfer data base required to develop heat transfer correlations and to assess computational fluid dynamic techniques for rotating coolant passages. An analysis of the governing equations showed that four parameters influence the heat transfer in rotating passages (coolant density ratio, Rossby number, Reynolds number and radius ratio). These four parameters were varied over ranges which exceed the ranges of current open literature results, but which are typical of current and advanced gas turbine engine operating conditions. Rotation affected the heat transfer coefficients differently for different locations in the coolant passage. For example, heat transfer at some locations increased with rotation, but decreased and then increased again at other locations. Heat transfer coefficients varied by as much as a factor of 5 between the leading and trailing surfaces for the same test condition and streamwise location. Comparisons with previous results are presented.

NOMENCLATURE

A	Cross sectional area of coolant passage
C_p	Specific heat of coolant
D	Hydraulic diameter
Gr	Rotational Grashof number
h	Heat transfer coefficient
k	Thermal conductivity
m	Mass flowrate
Nu	Nusselt number, hD/k
Pr	Prandtl number
Q	Heat flux
R	Radius
Re	Reynolds number, $\dot{m}D/\mu/A$
Ro	Rotation number, $\Omega D/V$
T	Temperature
V	Mean coolant velocity
x	Streamwise distance from inlet
$\Delta\rho/\rho$	Density ratio, $(\rho_b-\rho_w)/\rho_b$
Ω	Rotational speed
ρ	Coolant density
μ	Absolute viscosity

subscripts:

b	Local bulk condition
d	Outlet of system of heated surfaces
H	Constant heat flux
i	Inlet to coolant passage
u	Inlet to system of heated surface
w	Heated surface location
∞	Fully developed, smooth tube

superscripts:

-	Average

INTRODUCTION

In advanced gas turbine engines, increased speeds, pressures and temperatures are used to increase thrust/weight ratios and reduce the specific fuel consumption. As a result, the turbine blades are subjected to increased gas path temperatures in addition to increased levels of stress. Internal convection cooling is usually required to maintain acceptable airfoil metal temperatures and to obtain an acceptable blade life. Knowledge of the local heat transfer in the cooling passages and around the external blade surface is essential to predict blade metal temperatures. It has been demonstrated that rotation can significantly alter the local heat transfer in the internal coolant passages. Therefore, the turbine blade designer needs accurate local heat transfer predictions for blade coolant passages under conditions of rotation to effectively estimate blade life.

Predictions of heat transfer and pressure loss in airfoil coolant passages currently rely on correlations derived from the results of stationary experiments.

Presented at the Gas Turbine and Aeroengine Congress and Exposition—June 4-8, 1989—Toronto, Ontario, Canada
This paper has been accepted for publication in the Transactions of the ASME
Discussion of it will be accepted at ASME Headquarters until September 30, 1989

Adjustment factors are usually applied to these correlations to bring them into nominal correspondence with engine experience. This practice is unsatisfactory when blade cooling conditions for new designs lie outside the range of previous experience.

Heat transfer and pressure loss data are difficult and costly to obtain under conditions of rotation. As a consequence, there are limited amounts of data in the open literature that a turbine designer can use to account for the effects of rotation in typical turbine blade designs. The data that is available is far from comprehensive and is limited in scope.

Rotation of turbine blade cooling passages gives rise to Coriolis and buoyancy forces. Both of these forces can substantially affect coolant flow patterns which influence the heat transfer inside turbine blade cooling passages. The complex coupling of the Coriolis and buoyancy forces has prompted many investigators to study the secondary flows generated in unheated, rotating circular and rectangular passages without the added complexity of heat transfer and buoyancy. Much of the earlier work was conducted for laminar flow, because rig limitations (i.e., unpressurized passages) allowed only low Reynolds number flows with corresponding low rotation or Rossby numbers. The effects of rotation on secondary flow and stability have been investigated by Hart (1971), Wagner and Velkoff (1972), Moore (1967) and Johnston et al. (1972). These investigators have documented strong secondary flows and have identified aspects of flow stability in near-wall flow in rotating radial passages.

Buoyancy forces in gas turbine blades are substantial because of the high rotational speeds and large blade wall to coolant temperature differences. The effects of buoyancy on heat transfer without the complicating effects of Coriolis generated secondary flow have been studied in vertical stationary passages. Early experiments in this area were reported by Eckert et al. (1953), Metais and Eckert (1964) and Brundrett and Burroughs (1967). Flow criteria for forced-, mixed- and free-convection heat transfer was developed for parallel flow and counter flow configurations by Eckert (1953) and Metais (1964). Based on previous stationary combined-, free- and forced-convection experimental results and turbine blade operating conditions, buoyancy forces are expected to cause significant changes in the heat transfer in the rotating coolant passages.

The combined effects of Coriolis and buoyancy forces on heat transfer have been studied by a number of investigators. Heat transfer in rotating, smooth wall models has been investigated by Mori et al. (1971), Johnson (1978), Morris and Ayhan (1979), Lokai and Gunchenko (1979), Morris (1981), Iskakov and Trushin (1983) and, more recently, Guidez (1988). Large increases and decreases in local heat transfer were found to occur by some investigators under certain conditions of rotation while others showed lesser effects. Analysis of these results does not produce consistent trends in the effects of rotation on heat transfer. The disparity of the results is indicative of differences in the measurement techniques and models used in the experiments as well as the nonuniformity of the test conditions.

A comprehensive experimental program was formulated to identify the separate effects of Coriolis and buoyancy for the range of dimensionless heat transfer and flow parameters encountered in large aircraft gas turbines. The overall objective of the program was to acquire and correlate benchmark-quality local heat transfer and pressure loss data for multipass, rotating coolant passages under conditions similar to those expected in the first stages of advanced aircraft gas turbines. Heat transfer data were obtained under varying conditions of flowrate, rotation, model radius and wall-to-coolant temperature difference. The experiments were conducted by varying each parameter while holding the remaining parameters constant. The data was analyzed to separate the effects of Reynolds number, Coriolis forces, buoyancy, streamwise location and the geometric location in the coolant passage (i.e., leading or trailing surfaces).

The results presented in this paper are from the first phase of a three phase program which studied the effects of rotation on a multipass model with smooth and rough wall configurations. The first phase utilized the smooth wall configuration. Subsequent phases will include normal and skewed trip geometries. This paper presents heat transfer results obtained in the first, radially outward flowing passage of a four-pass, smooth wall, square passage model. The results will show 1) agreement with previous investigators for stationary conditions, 2) effects of Coriolis forces which cause the leading and trailing side heat transfer to vary by factors as large as five and 3) effects of buoyancy which cause heat transfer to increase by as much as a factor of two.

DESCRIPTION OF EXPERIMENTAL EQUIPMENT

Rotating Heat Transfer Facility

The experimental facility consists of the containment vessel with rotating arm assembly and a motor with controller (Figure 1). The containment vessel is 6 ft (1.83 m) in diameter. The vessel was designed for operation at pressures as low as 5 mm of Hg. absolute to reduce the power required to rotate the arm. The rotating arm assembly was turned by a 15 HP DC motor via a toothed belt. Shaft RPM was controlled by an adjustable feed back electronic controller. For this series of experiments, shaft speed was varied from 0 to 1100 RPM producing maximum gravitational forces on the model of approximately 1100g at the tip of the model and approximately 800g at the root.

The shaft assembly is comprised of a main outer shaft with two shorter inner shafts. This shaft arrangement was designed for dual fluid paths from each

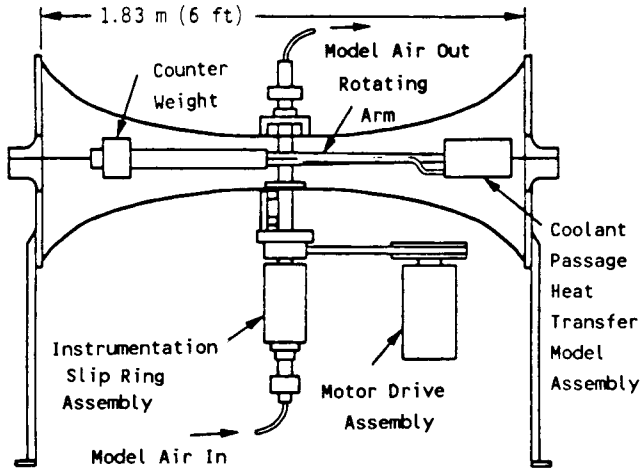

Fig. 1 Rotating Heat Transfer Facility

rotary union mounted on the ends of the shaft to the rotating assembly. The rotary unions had carbon faced seals and were tested at assembly to be "bubble tight" to 150 psia (1034 kPa). The total leakage rate through all the components in stationary tests was less than 0.2 percent of the baseline flow rate. Grooves located on the exterior surface of the outer shaft allow instrumentation and power leads to extend from the rotating arm to the rotating portion of the instrumentation slipring. Two slipring assemblies (a 40 channel unit located on the upper end of the shaft and a 200 channel unit located on the lower end of the shaft) were used to transfer heater power and instrumentation leads between the stationary and rotating frames of reference.

Heat Transfer Model

The heat transfer model was designed to simulate the multi-passage geometry of an internally cooled turbine blade (Figure 2). The model consists of three heated straight sections, three heated turn sections and one unheated straight section as shown in Figure 3. All data presented herein were obtained in the first heated passage with radially outward flow. The model passages are square with a sidewall dimension of 0.5 in. (12.7 mm). The heated length of the first passage is 14 hydraulic diameters and is comprised of sixteen heated copper elements at four streamwise locations. Four elements form the walls of the square coolant passage at each streamwise location. The two cross section views shown in the figure show the orientation of the leading, trailing and side wall surfaces. Each copper element is heated on the side opposite the test surface with a thin-film, 0.003 in. (0.1 mm), resistance heater. Each element is 0.150 in. (3.8 mm) thick and is thermally isolated from surrounding elements by 0.060 in. (1.5 mm) thick fiberglass insulators. The power to each element was adjusted to obtain an isothermal wall boundary condition. The heat flux between elements with a 2F (1C) temperature difference was estimated to be less than 2 percent of a typical stationary heat flux from a test element. The combination of distributed heating on the back of the copper element and the thickness of the element produced an almost uniform (<2F) temperature element.

The heat transfer model was operated at nondimensional flow conditions typical of current and advanced gas turbine designs. The required nondimensional rotation numbers were obtained with rotation rates of 1100 RPM or less by operating the model at a pressure of approximately 10 atmospheres. The inlet coolant temperature was typically 80F (27C) and the copper test surface elements were 120F, 160F, 200F and 240F (49C, 71C, 93C and 116C) for coolant-to-wall temperature differences of 40F, 80F, 120F and 160F (22C, 44C, 67C and 89C). Temperatures of the copper elements were measured with two chromel-alumel thermocouples inserted in drilled holes of each copper element. Heat transfer coefficients were obtained for each heated surface location by the method described below.

Data Reduction

Data acquisition/analysis consisted of two tasks: determination of the conduction back-loss of the model and the determination of the heat transfer coefficients. Model back-loss measurements were obtained with no coolant flow and uniform wall temperature under steady-state conditions with rotation, identical to the heat transfer experiments, but without coolant flow. The model back-losses in the first passage ranged from 10 to 20 percent of the total heat generated for stationary heat transfer levels. Heat transfer coefficients were determined for each wall section by applying an energy balance on each heated surface. The net heat added to the coolant by convection was determined from the electrical power used to heat each surface less the heat conducted from the element to the model support structure.

The coolant temperature was determined with a thermodynamic energy balance through each set of heated surfaces. The mean bulk temperature was determined by marching along the test section and calculating the temperature rise due to the net heat addition to the coolant. The calculation was started at the inlet of the coolant pasage where the coolant temperature was measured. The average coolant temperature for each heated surface was determined by averaging the inlet and exit calculated bulk temperatures for each set of four heated surfaces.

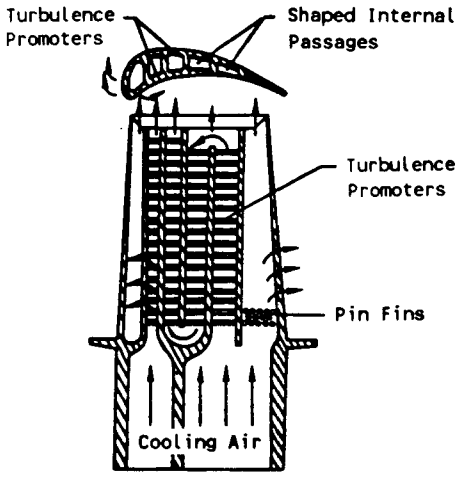

Fig. 2 Typical Turbine Blade Internal Convection - Cooling Configuration (from Han et al., 1984)

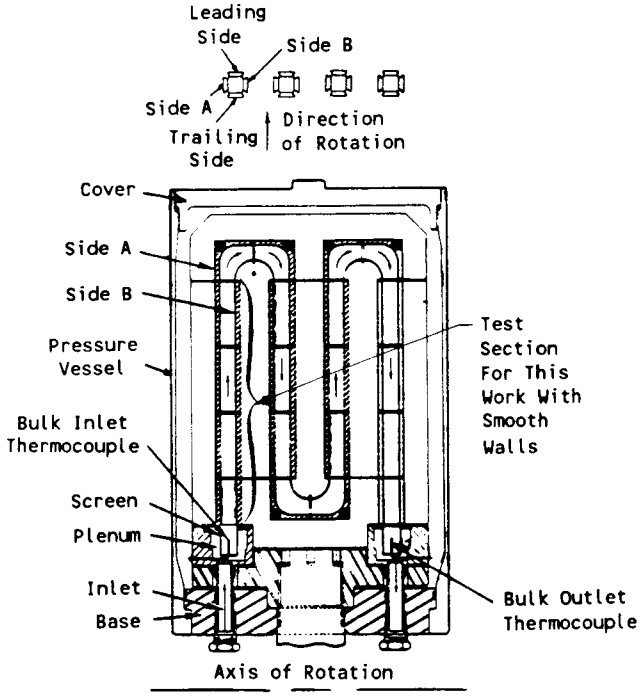

Fig. 3 Cross Sectional Views of Coolant Passage Heat Transfer Model Assembly

$$T_d = \Sigma Q_{net}/(\dot{m}C_p) + T_u \quad (1)$$

where Q_{net} is the convective heat flux from each of the four test surfaces at the specific streamwise location.

Variations of coolant bulk temperature relative to the typical inlet coolant temperature of 80F are shown in Figure 4 for rotation numbers of 0.0 and 0.48. The shaded symbols are the calculated coolant temperatures from "Eq. 1". The open symbols are the average coolant and wall temperatures for each element. The uncertainty of the measurement of temperature is estimated to be ±2.5F (±1.4C).

The average heat transfer coefficient for each element was determined by dividing the net heat input to the coolant by the projected heated surface area and the temperature difference between the average heated surface temperature and the calculated average coolant bulk temperature.

$$h = \frac{Q_{net}}{\text{Surface Area} * (\bar{T}_w - \bar{T}_b)} \quad (2)$$

Dimensionless heat transfer and flow parameters were calculated for each element (e.g. Nu and Re). The properties in the Nusselt and Reynolds number were evaluated at the film temperature, i.e., $T_f = (\bar{T}_w + \bar{T}_b)/2$. All of the heat transfer results presented herein have been normalized with a smooth tube correlation for fully developed, turbulent flow. The constant heat flux Colburn equation adjusted for constant wall temperature was used to obtain the Nusselt number for fully developed, turbulent flow in a smooth tube (Kays and Perkins, 1973).

$$Nu_H = 0.022 * Re_d^{0.8} * Pr^{0.6} \text{ (Colburn Equation)} \quad (3)$$

with Pr = 0.72

$$Nu_\infty = 0.0176 * Re_d^{0.8} \quad (4)$$

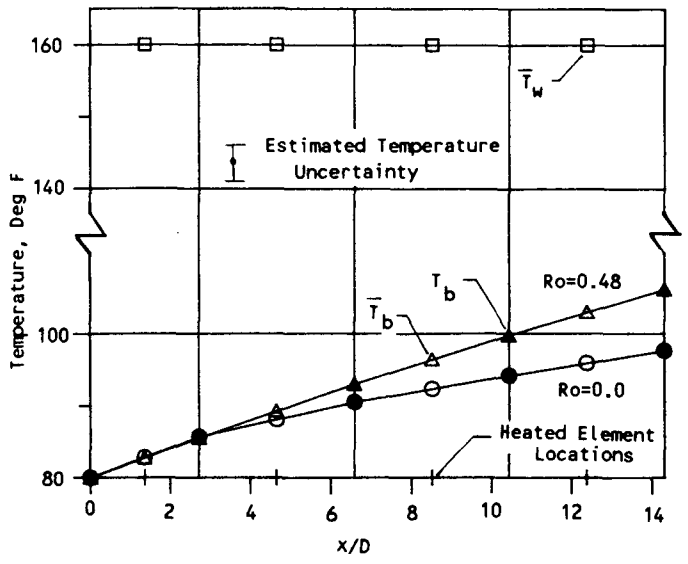

Fig. 4 Variation of Coolant Bulk Temperature with Streamwise Location; Re = 25000, $(\Delta\rho/\rho)_i$ = 0.13

An uncertainty analysis of the data reduction equations showed that approximately 3/4 of the estimated uncertainty in calculating heat transfer coefficient was due to the temperature measurement. Estimates of the uncertainty in calculating heat transfer coefficient typically varied from approximately ±6% at the inlet to ±8% at the exit of the first passage of the heat transfer model for the baseline test condition. The uncertainty of the heat transfer coefficient is influenced mainly by the wall-to-coolant temperature difference and the net heat flux from each element. Uncertainty in the heat transfer coefficient increases when either the temperature difference or the net heat flux decreases. For increasing x/D, the uncertainty increases because the wall-to-coolant temperature difference decreases (see Figure 4). For low heat fluxes (e.g., for low Reynolds numbers and on the leading surfaces with rotation) the uncertainty in the heat transfer coefficient increased. The uncertainty in the lowest heat transfer coefficient on the leading side of the passage with rotation was estimated to be 20 percent.

Coolant Passage Inlet Documentation

Velocity and turbulence measurements were obtained at the exit of the screen assembly (inlet of the coolant passage, see Figure 3) for a Reynolds number of 15,000 with no rotation. For these measurements, the four legged duct was removed from model. The measurements were obtained by traversing a hot film probe across the 0.5 by 0.5 in. (12.7 by 12.7 mm) opening downstream of the coolant inlet assembly. Average and RMS voltages from the linearized hot film signal were used to determine the local mean velocity and local turbulence intensity. The mean velocity and turbulence intensity results for the flow from the exit of the screen assembly (entrance to the coolant passage) are shown in Figure 5. The inlet screen system was designed to produce an inlet velocity profile which is similar to that for a fully developed turbulent pipe flow. The mean velocity profiles have an approximately parabolic shape but are slightly skewed toward the outside (side A) and trailing side of the passage. Turbulence profiles at the exit of the screen assembly show increases in local turbulence intensity near the edges of the flow with a centerline turbulence level of

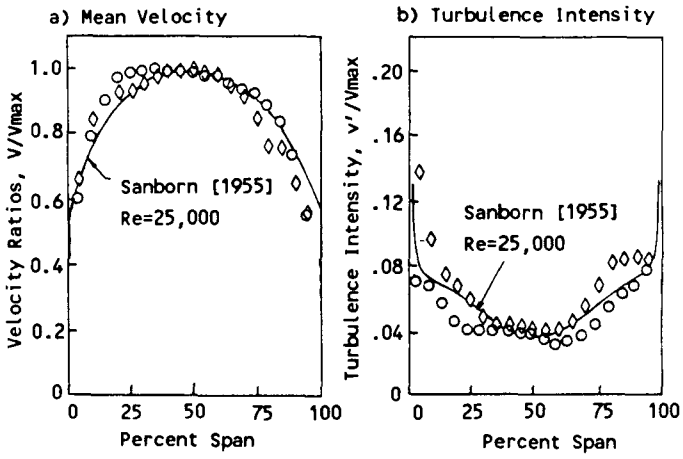

Fig. 5 Mean Axial Velocity and Turbulence Intensity Profiles at Heat Transfer Passage Inlet Plane; Re = 15,000, Ω = 0, ○ - plane through axis of rotation, ◇ - plane perpendicular to axis of rotation

approximately four percent. The mean velocity and turbulence profiles are in good agreement with those from Sandborn (1955) for fully developed pipe flow. The effects of rotation on the inlet velocity distribution are not known. However, an analytical study is being initiated to determine the effects of rotation on the inlet velocity distribution and results will be reported at a future date.

RESULTS

Heat transfer in stationary experiments with smooth passages is primarily a function of the Reynolds number (a flow parameter) and the streamwise distance from the inlet, x/D (a geometric parameter). However, when rotation is applied, the heat transfer is also strongly influenced by the coupled effects of Coriolis and buoyancy and becomes asymmetric around the passage. An unpublished analysis of the equations of motion by Suo (1980), similar to that of Guidez (1988), showed that the basic nondimensional fluid dynamic parameters governing the flow in a radial coolant passage were the Reynolds number, the rotation number, $\Omega D/V$, fluid density ratio, $\Delta\rho/\rho$, and the geometric parameter, R/D. (Note that the rotation parameter is the reciprocal of the Rossby number, $V/\Omega D$.) The rotation number, $\Omega D/V$, the fluid density ratio, $\Delta\rho/\rho$, and the geometric parameter, R/D, can be combined to form a buoyancy parameter $(\Delta\rho/\rho)(R/D)(\Omega D/V)^2$. This combined parameter influences the formation of both cross-stream and buoyancy driven secondary flow and, consequently, also influences the heat transfer. Thus, with rotation, the heat transfer is primarily a function of two geometric parameters (x/D and surface orientation relative to the direction of rotation) and three flow parameters (Reynolds number, rotation number and buoyancy parameter).

The effect of each of the five parameters on the heat transfer is difficult to determine when most of the parameters influence the heat transfer by similar amounts. Our approach to developing understanding of the cause/effect relationships is, first, to show the effects of each primary variable about a baseline flow condition and then, second, to examine our entire body of experimental results to determine regimes where each of the three flow parameters dominates the heat transfer.

Baseline Experiments

Two baseline experiments, one stationary and one rotating, were conducted to obtain data for comparison with all other data generated in this program. The stationary and rotating baseline experiments had nondimensional flow conditions which consisted of a Reynolds number of 25,000 and an inlet density ratio, $(\Delta\rho/\rho)_i = (T_w-T_b)/T_w$, of 0.13. The rotating baseline experiment had a rotation number, $\Omega D/V$, of 0.24 and a radius ratio at the average model radius, $\bar{R}/D$, of 49. These parameters were selected because they are in the central region of the operating ranges of current large aircraft gas turbine engines.

Stationary - The streamwise distribution of the average heat transfer ratio for the stationary (and very low rotation rate) baseline experiments are shown in Figure 6. The wall-to-wall variation of the heat transfer results from the four surfaces around the circumference of the coolant passage are also shown. Results from other investigators (Boelter et al., 1948, Aladyev, 1954, and Yang and Liao, 1973) are shown for comparison.

The streamwise variations in average heat transfer ratio are indicative of developing flow in the entrance region of a passage. Note that the heat transfer ratio decreases from over 2.0 near the inlet of the first passage to about 1.0 near the exit. A heat transfer ratio of 1.0 is that expected for fully developed, turbulent flow with a constant wall temperature. Although the mean inlet velocity profiles were conditioned to be hydrodynamically "fully developed" for a circular passage, the heat transfer results indicate that an additional development process occurs along the passage length. This development is attributed to thermal and near-wall flow development as well as the hydrodynamic development of flow in a square cross-section passage. The wall-to-wall variation in heat transfer ratio for each streamwise location is less than 15 percent, indicating good passage symmetry. The wall-to-wall variation was random in nature except at $\bar{x}/D = 12.4$, where the wall-to-wall variation was judged to be systematic. The greatest wall-to-wall difference in heat transfer ratio occurred at $\bar{x}/D = 12.4$ and was attributed to upstream effects of the turn. In general, consistent wall-to-wall heat transfer results were obtained.

Rotating - The streamwise distributions of heat transfer ratio for the rotating baseline condition for the four surface locations around the coolant passage are shown in Figure 7. The streamwise distribution of the average heat transfer ratio from all four surfaces from the stationary baseline test is also shown.

With rotation heat transfer increases and decreases by factors of more than two from the trailing and leading surfaces, respectively, compared to the heat transfer from the stationary model. The heat transfer from the sidewall surfaces increases by factors of 1.2 to 1.5. Note that the local heat transfer ratio on the leading side of the coolant passage decreases rapidly with increasing streamwise distance to about 40 percent of the stationary value at $\bar{x}/D = 8.5$ and then increases

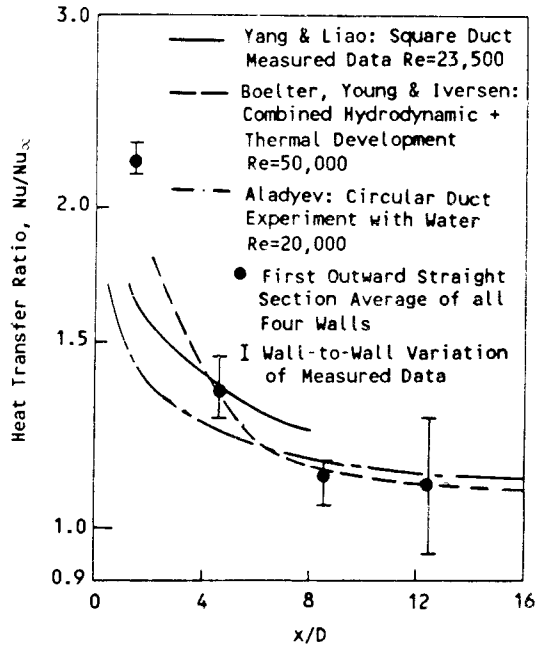

Fig. 6 Variation of Heat Transfer with Streamwise Location for "Nonrotating" Baseline Flow Conditions; Re = 25000, $(\Delta\rho/\rho)_i = 0.13$ average of Ω = -15, 0, +15 RPM; Ro = 0.006

at the larger x/D location. The heat transfer ratio on the trailing side increases with increasing streamwise distance to almost 2.5 times that of a fully developed, smooth tube. This results in a 6-to-1 ratio of the heat transfer coefficients between the trailing and leading surfaces.

The difference in heat transfer between the rotating and nonrotating flow conditions on the trailing and sidewall surfaces is attributed to both the increasing strength of the secondary flow cells associated with the Coriolis force and the buoyancy. The decrease in heat transfer near the inlet of the passage on the leading surfaces is attributed to the stabilizing of the near-wall flow, as observed by Johnston (1972). The subsequent increase in heat transfer near the end of the passage is postulated to occur when the secondary flow cells become more developed and interact with the buoyant, stabilized near-wall flow on the leading side of the passage. Further discussion of this interaction will be presented in subsequent sections. The heat transfer effects described above are characteristic of radially outward flow in rotating passages and are attributed to the combined Coriolis and buoyancy forces.

As noted above in the discussion of the baseline results, rotation significantly changes the heat transfer from the leading and trailing surfaces but causes smaller changes on the sidewall surfaces. Therefore, the following discussion will focus on the heat transfer results from only the leading and trailing surfaces.

Varying Rotation Number

The rotation number, $\Omega D/V$, was varied from 0 to 0.48 for this series of flow conditions. The Reynolds number, inlet density ratio and radius ratio were held constant at the nominal values of 25,000, 0.13 and 49, respectively.

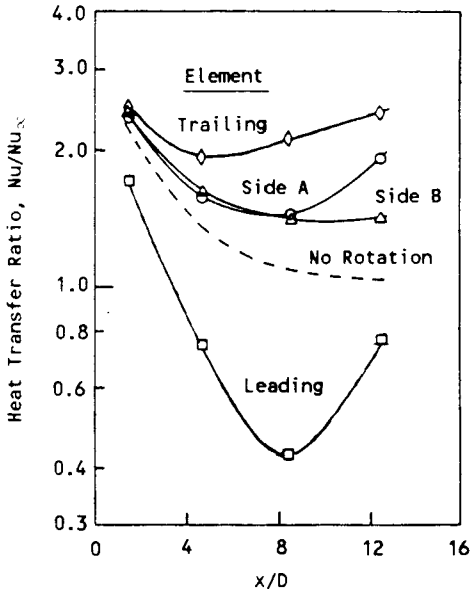

Fig. 7 Variation of Heat Transfer Ratio with Streamwise Location for "Rotating" Baseline Flow Condition; Re = 25000, Ro = 0.24, $(\Delta\rho/\rho)_i$ = 0.13

Trailing Surfaces - Increasing the rotation rate causes significant increases in heat transfer on the trailing surfaces (Figure 8a). As the rotation parameter is increased from 0 to 0.12, the heat transfer ratio increases more than 50 percent above the stationary values in the latter half of the coolant passage and only slightly in the first half. As rotation is further increased, the heat transfer ratio increases over the whole passage length to values of almost four for the rotation number of 0.48.

The large increases in the heat transfer ratio in the latter half of the passage for low rotation numbers are attributed to the development of Coriolis generated secondary flow cells. The general increase in heat transfer ratio on the entire trailing side of the passage for larger rotation numbers is attributed to the upstream movement of the onset and the increasing strength of these secondary flow cells. The coolant near the trailing side of the passage (high pressure side for radially outward flow) is also believed to be influenced by the destabilization of the wall shear layers due to rotation. Additionally, cooler mainstream fluid is accelerated towards this side of the passage by the Coriolis forces. The large increases in the heat transfer from the trailing surfaces are attributed to a combination of these effects.

Leading Surfaces - Heat transfer from the leading surfaces is also strongly influenced by rotation (Figure 8b). However, the effect of rotation is markedly different from that observed on the trailing surfaces. In contrast to the continual increase in heat transfer with increasing rotation number on the trailing side, the heat transfer ratio decreases with increasing rotation number on the leading side of the passage near the inlet. For all of the remaining locations on the leading side of the passage, the heat transfer ratio decreases and then increases again with increasing rotation number. Examination of the leading side results shows that the location of the local minimum in the heat transfer ratio for each rotation number moves toward the inlet of the passage as the rotation number is increased.

Significantly lower heat transfer rates were measured along the leading side of the coolant passage for even low values of rotation numer. The decreases in the heat transfer ratio are attributed, for the most part, to the cross-stream flow patterns in the passage as well as the stabilization of the flow near the leading side of the passage (discussed in the previous section). The cross-stream flows cause already heated, relatively quiescent fluid from the trailing and sidewall surfaces to accumulate near the leading side of the coolant passage. In addition, the rotation stabilizes the shear layers along this wall and further reduces the potential for heat transfer from turbulent transport. The increase in the heat transfer ratio in the latter half of the coolant passage for the larger rotation numbers is attributed to the large scale development of the Coriolis generated secondary flow cells.

Varying Density Ratio

The inlet density ratio, $(\Delta\rho/\rho)_i$, was varied from 0.07 to 0.22 for this series of flow conditions. The Reynolds number, rotation number and radius ratio were held constant at the nominal values of 25,000, 0.24 and 49, respectively.

Increasing the inlet density ratio (i.e., the wall-to-coolant temperature difference) from 0.07 to

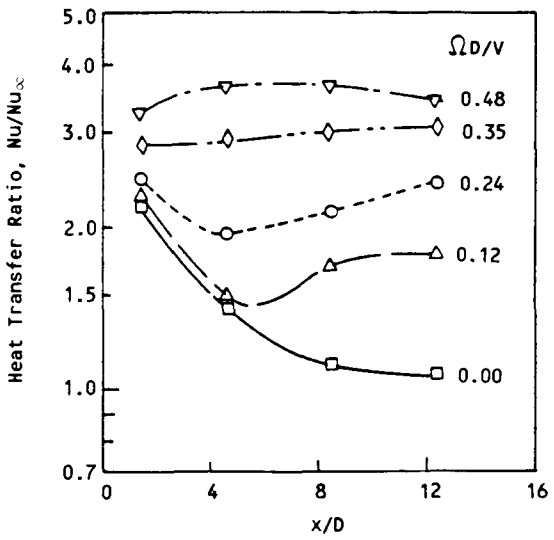

Fig. 8a Effect Of Rotation Number on Heat Transfer Ratio for Trailing Surfaces; Re = 25000, $(\Delta\rho/\rho)_i$ = 0.13, $\overline{R}/D$ = 49

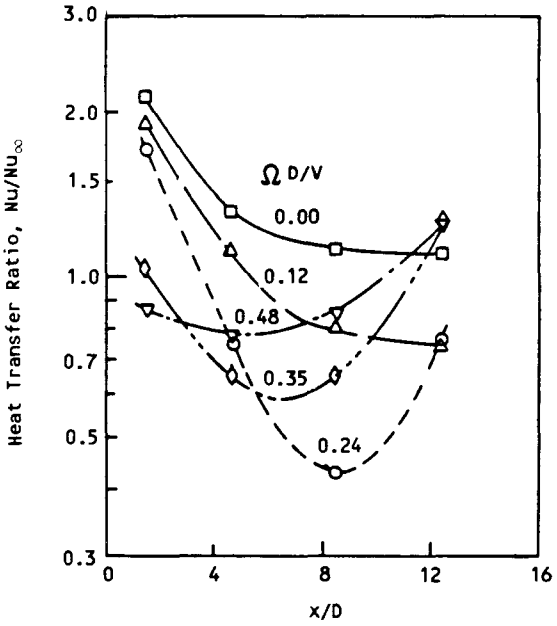

Fig. 8b Effect of Rotation Number on Heat Transfer Ratio for Leading Surfaces; Re = 25000, $(\Delta\rho/\rho)_i$ = 0.13, $\overline{R}/D$ = 49

0.22 causes the heat transfer ratio to increase on all trailing surfaces by as much as 50 percent and on the two downstream leading surfaces by as much as 100 percent (Figure 9). The largest increases in heat transfer with increasing density ratio are in areas of the passage where the effects of Coriolis are also strong. The exception to the general increase in heat transfer with increasing density ratio occurred near the inlet on the leading side of the passage, where the heat transfer ratio is observed to decrease slightly. The heat transfer for this particular location, as noted above, is relatively unaffected by the Coriolis generated secondary flow for this rotation number and is believed to be dominated by near-wall flow stabilization. Increasing the density ratio in this region adds an additional stabilizing effect due to the opposing signs of the buoyancy force and the direction of the mainstream flow. This localized decrease in heat transfer ratio is also consistent with the results of Morris (1979), (1981) who found a decrease in heat transfer on leading surfaces with increasing Grashof number (i.e., either increasing density ratio and/or increasing rotation number). This decrease was observed by Morris at values of rotation number of approximately 0.05.

Varying Reynolds Number

The Reynolds number was varied from 12,500 to 50,000 for this series of flow conditions. The rotation number, inlet density ratio and radius ratio were held constant at the rotating baseline values of 0.24, 0.13 and 49, respectively.

The streamwise distributions of heat transfer ratio for three Reynolds numbers are shown in Figure 10. For these tests, the coolant mass flowrate, $\dot{m}$, and rotation rate, Ω , were varied to maintain a constant rotation number of 0.24. Changing the Reynolds number about the rotating baseline condition yielded a variation of heat transfer ratios with streamwise location which were similar to those for the rotating baseline flow condition. There is no consistent trend in the heat transfer results with variations in the Reynolds number for this rotation number. However, there is a significant decrease in heat transfer ratio with increasing Reynolds number on the leading side of the passage at the most downstream location, $\overline{x}/D$ = 12.4.

Varying Model Radius

In order to isolate the effect of the radius ratio, $\overline{R}/D$, the mean model radius was decreased to about two-thirds of its baseline value (from $\overline{R}/D$ = 49 to 33). The Reynolds number, rotation number and inlet density ratio were held constant at the baseline values of 25,000, 0.24 and 0.13, respectively.

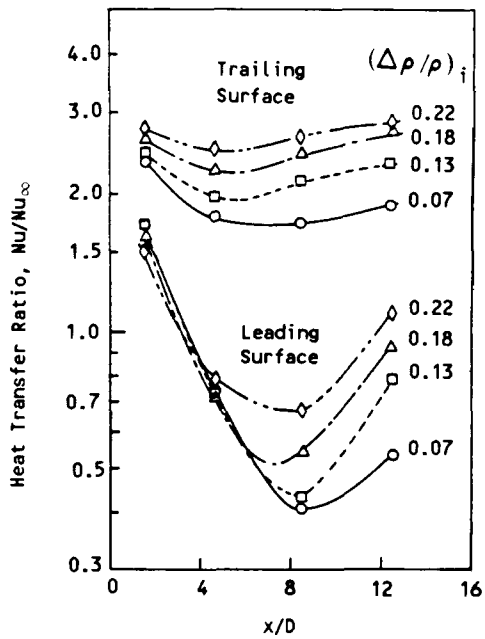

Fig. 9 Effect of Wall-to-Coolant Density Difference on Heat Transfer Ratio; Re = 25000, Ro = 0.24, $\overline{R}/D$ = 49

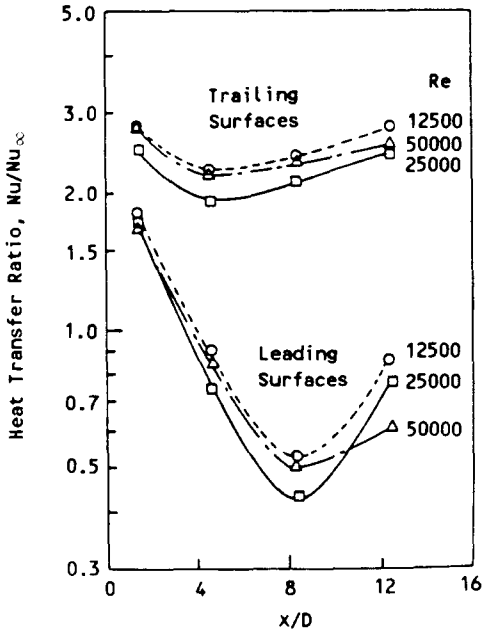

Fig. 10 Effect of Reynolds number on Heat Transfer Ratio: Ro = 0.24, $(\Delta\rho/\rho)_i$ = 0.13, $\bar{R}/D$ = 49

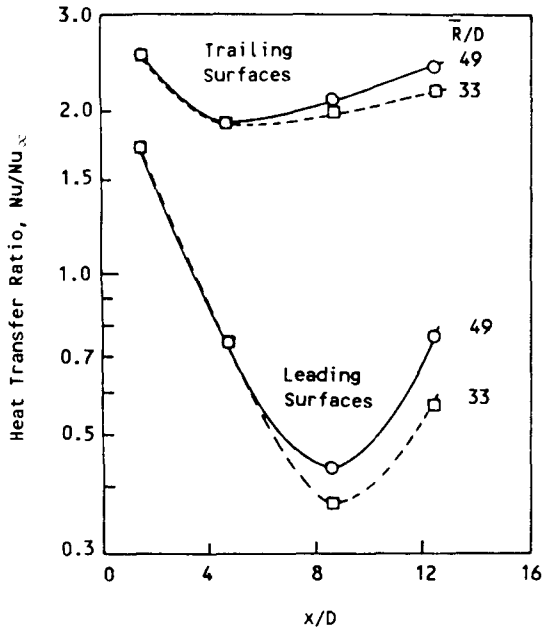

Fig. 11 Effect of Model Radius on Heat Transfer Ratio Distribution; Re = 25000, Ro = 0.24, $(\Delta\rho/\rho)_i$ = 0.13

The effects of decreasing the model radius on the heat transfer ratio are shown in Figure 11. Heat transfer ratios near the inlet of the passage on both the leading and the trailing surfaces are relatively unaffected by the radius change. However, the heat transfer ratio did decrease with a decrease in model radius in the latter half of the passage. These results are similar to those discussed above where density ratio was decreased from the baseline value of 0.13 to 0.07. Because the effects of buoyancy are coupled as the product of two flow parameters and one geometric parameter into a combined buoyancy parameter: $(\Delta\rho/\rho)(R/D)(\Omega D/V)^2$, varying the density ratio or the radius ratio by similar amounts should cause similar variations in the heat transfer distributions.

Varying Rotation Number and Density Ratio

Additional data from parametric variations of density ratio and rotation parameter were necessary to isolate the effects of rotation and buoyancy. The inlet density ratio was varied from 0.07 to 0.22 for selected rotation numbers. Heat transfer results from these experiments were plotted vs. inlet density ratio with rotation number as a secondary variable. The distributions of heat transfer ratio with density ratio (not shown) were extrapolated for each value of the rotation number to obtain a value of the heat transfer ratio for a density ratio of 0.0 (i.e., limit as ΔT approaches 0). The heat transfer results obtained from the experiments plus the extrapolated values for a density ratio of 0.0 are presented in Figure 12 as the variation of heat transfer ratio with the rotation number with the density ratio as the secondary variable for three streamwise locations.

Trailing Surfaces - The heat transfer ratios for the trailing surfaces increase with increases in either the density ratio or the rotation number. The heat transfer from the two downstream surfaces on the trailing side increases by a factor of almost two as density ratio increases from 0 to 0.22 at values of rotation number from 0.18 to 0.35. Note that there is no effect of density ratio on the heat transfer ratio for a rotation number of 0 when film properties are used for the dimensionless heat transfer and flow parameters. Increasing the rotation number causes local increases in the heat transfer by factors as much as 3.5 compared to the heat transfer for a rotation number of 0. The trend (but not the magnitude) for continuously increasing heat transfer coefficients with increasing density ratio and rotation number is consistent with the combined free and forced convection results of Eckert et al. (1953) and Metais and Eckert (1964) where the buoyancy force direction is opposite to the mean flow direction as it is for radially outward flowing rotating passages. However, the flow in the present experiment with rotation is more complicated than the flow in stationary experiments because all surfaces do not behave in a similar manner.

Leading Surfaces - The heat transfer from the leading surfaces is more complex than that from the trailing surfaces. Heat transfer decreases with increasing rotation number for low values of rotation number (i.e., $\Omega D/V < 0.2$ at the downstream location) and then subsequently increases again with increases in rotation for larger values of rotation number. Additionally, as with the trailing surfaces, heat transfer increases with increases in the density ratio. The more complicated heat transfer distributions on the leading side of the coolant passage are attributed to 1) the combination of buoyancy forces and the stabilization of the near-wall flow for low values of the rotation number and 2) the developing, Coriolis driven secondary flow cells for the larger values of the rotation number.

Variations in the absolute and relative changes of the heat transfer coefficients on the leading and trailing surfaces can be deduced from the results shown in Figure 12. The relative increase in heat transfer ratio for the downstream location on the leading side is greater than 3 as the inlet density ratio is increased

from 0 to 0.22 for a rotation number of 0.25. However, note that the absolute increase in the heat transfer ratio is 0.8. This absolute increase is substantially less that the absolute increase in the heat transfer ratio from the trailing side for this rotation number and same increase in inlet density ratio (approximately 1.3). The difference in the increase in heat transfer ratio for the same increase in inlet density ratio suggests that the interaction of the Coriolis and buoyancy effects is different for the leading and trailing surfaces, even where the effects of Coriolis driven secondary flows are strong.

CORRELATING PARAMETERS

The analysis of the equations of motion for flow in a rotating radial passages by Suo (1980), discussed above, showed that 1) the variations in the momentum of the flow in the plane perpendicular to the passage centerline (cross-stream flow) will be proportional to the rotation number, $\Omega D/V$, and 2) the variations in the momentum of the flow parallel to the passage centerline (buoyant flows) will be proportional to the buoyancy parameter, $(\Delta\rho/\rho)(R/D)(\Omega D/V)^2$. The buoyancy parameter defined above is equivalent to the ratio of the Grashof number (with a rotational gravitation term, $R\Omega^2$) to the square of the Reynolds number and has previously been used to characterize the relative importance of free- and forced-convection in the analysis of stationary mixed-convection heat transfer. Guidez (1988) used a similar analysis to establish appropriate flow parameters for the presentation of his results. These parameters, $\Omega D/V$ and $(\Delta\rho/\rho)(R/D)(\Omega D/V)^2$, will also be used in the present discussion of the effects of Coriolis and buoyancy forces on the heat transfer.

The data and extrapolated results presented in Figure 12 show that the effects of Coriolis and buoyancy forces are coupled through the entire operating range investigated. The results from Figure 12 combined with those for $\overline{R}/D = 33$, are presented in Figure 13 as the variation of the heat transfer ratio with the buoyancy parameter. The local density ratio and radius, R, are used in the buoyancy parameter. Thus, the range of the buoyancy parameter decreases with incresing values of x/D. Results for the same value of the rotation number are connected with dashed lines where the results are not well correlated by the buoyancy parameter. The lines at constant rotation number are extrapolated to the value of the heat transfer ratio estimated for a density ratio (and also buoyancy parameter) of 0 as described in the discussion of Figure 12.

The heat transfer ratios for the trailing side of the passage increase with the buoyancy parameter. The rate of increase in the heat transfer ratio with increasing buoyancy parameter is greatest at the $\overline{x}/D = 12.4$ location for values of buoyancy parameter less than 0.4. For values of the buoyancy parameter greater than 0.4, the rate of increase is less. Thus, two ranges of buoyancy parameter appear to exist with different heat transfer characteristics. Generally, the heat transfer variations from the trailing side form a one-to-one

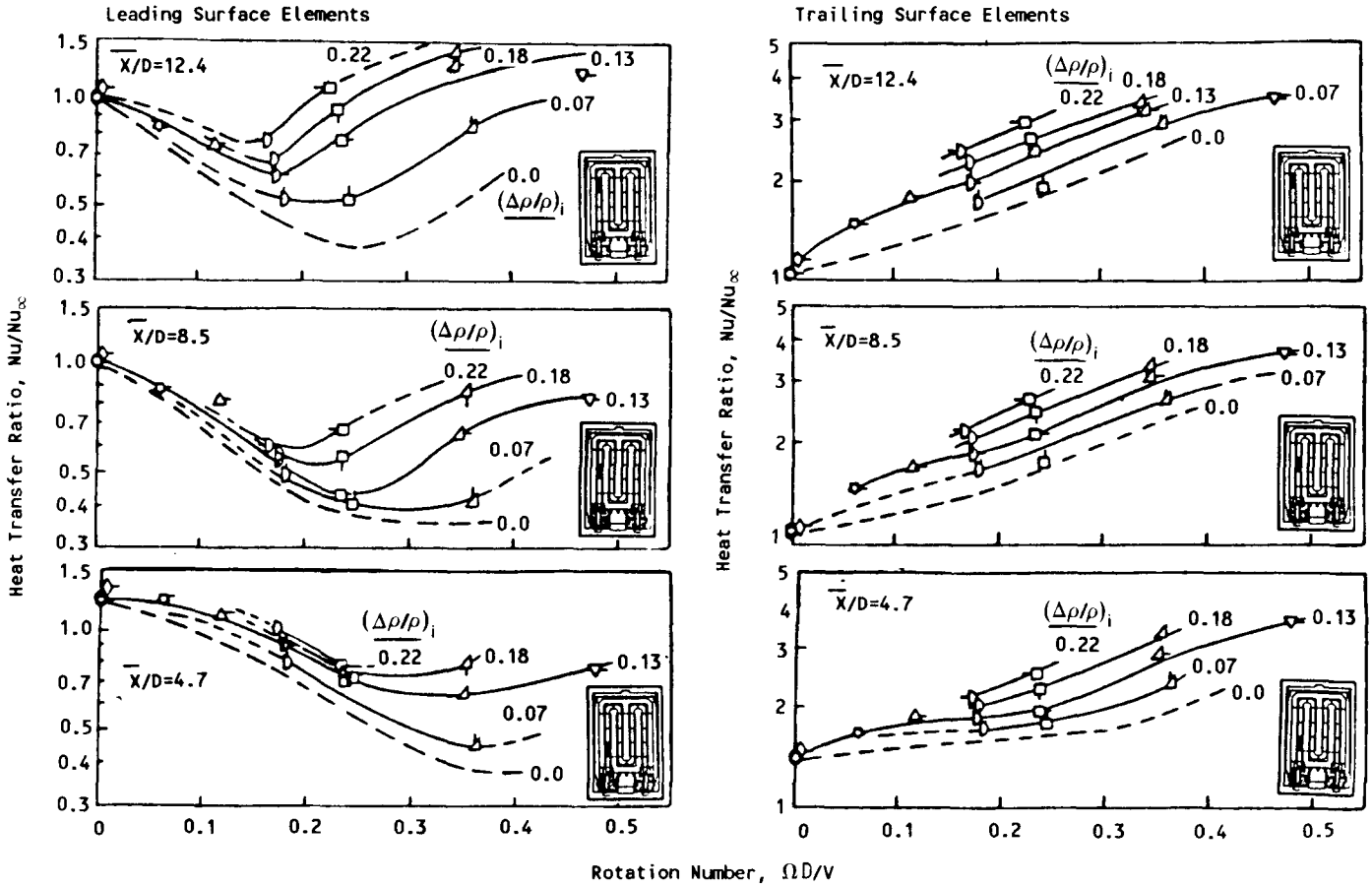

Fig. 12 Variation of Heat Transfer Ratio With Rotation Number at Selected Density Ratios and Streamwise Locations; Re = 25000, $\overline{R}/D = 49$

correspondence with the buoyancy parameter (i.e., singled valued function) and are well correlated by the buoyancy parameter for all values of $\overline{x}/D$ shown.

Examination of the heat transfer results from the leading side suggest that at least three ranges of buoyancy parameter exist where the heat transfer is dominated by different fluid dynamic mechanisms (i.e., Coriolis, buoyancy, etc.). Comparing the results at $\overline{x}/D$ = 12.4 from the leading side with those from the trailing side, note that there is a range of buoyancy parameter for values less than 0.1 where the heat transfer ratios decrease sharply with increasing values of the buoyancy parameter. Within the second range from 0.1 to approximately 0.5, the heat transfer ratios increase sharply with increasing values of the buoyancy parameter. For the third range, with values of the buoyancy parameter greater than 0.5, the heat transfer ratio increases at a lower rate, with increasing values of buoyancy parameter. For lower values of $\overline{x}/D$, the values of buoyancy parameter which define the limits of the three ranges, increase in magnitude. The heat transfer on the leading surface at values of $\overline{x}/D$ = 4.7 and 8.5 is governed by a more complex relationship of streamwise distance, rotation number and buoyancy parameter. However, the results from the leading side for $\overline{x}/D$ = 12.4 are well correlated by the buoyancy parameter for values of the buoyancy parameter greater than 0.2.

The analyses of these heat transfer results show that 1) the buoyancy parameter correlates the heat transfer ratio data from the trailing side of the coolant passage and from the leading side at the downstream location, 2) the data was not correlated by the buoyancy parameter near the inlet on the leading surface due to a complex interaction of stabilization, buoyancy forces and Coriolis effects, and 3) the heat transfer in rotating, smooth passages is governed by complex interactions of the viscous, Coriolis and buoyancy forces on the fluid.

COMPARISON WITH PREVIOUS EXPERIMENTAL RESULTS

The heat transfer results from the leading surface at $\overline{x}/D$ = 12.4 are compared in Figure 14 with the correlation from Morris (1981). Morris' experiment consisted of a rotating circular tube with radially outward flow with constant wall heat flux. The solid lines on the figure indicate the range of Morris' data, while the dashed lines represent extrapolations of his correlation. The heat transfer results (and symbols) shown in the figure are identical to those in Figures 12 and 13 for the leading surface elements with $\overline{x}/D$ = 12.4. The heat transfer results obtained on the leading surface at the low rotation number of 0.06 are within 20 percent of Morris' correlation. This agreement occurs

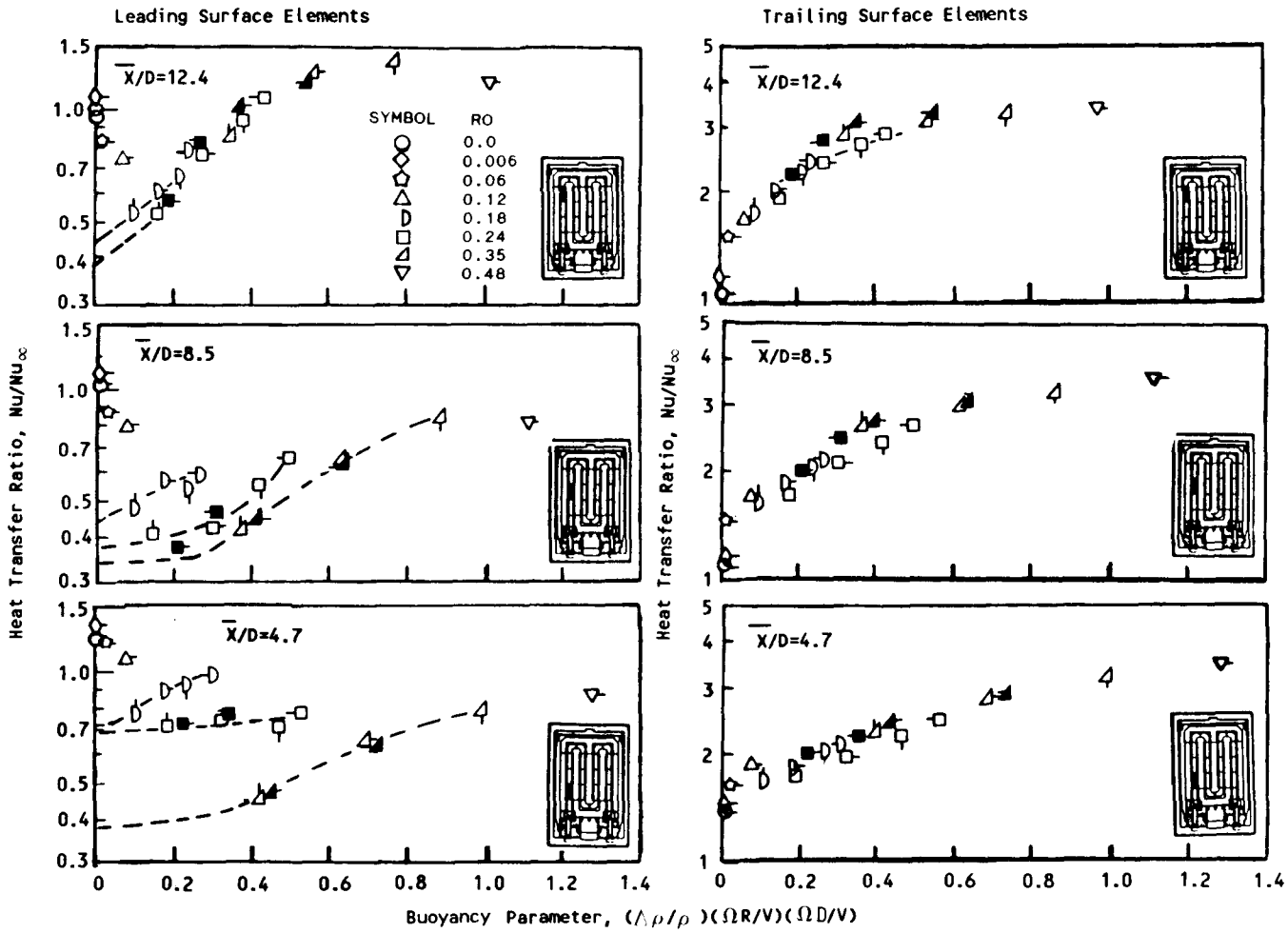

Fig. 13 Variation of Heat Transfer Ratio With Buoyancy Parameter; Re = 25000, $\overline{R}/D$ = 49 - open symbols, R/D = 33 - shaded symbols

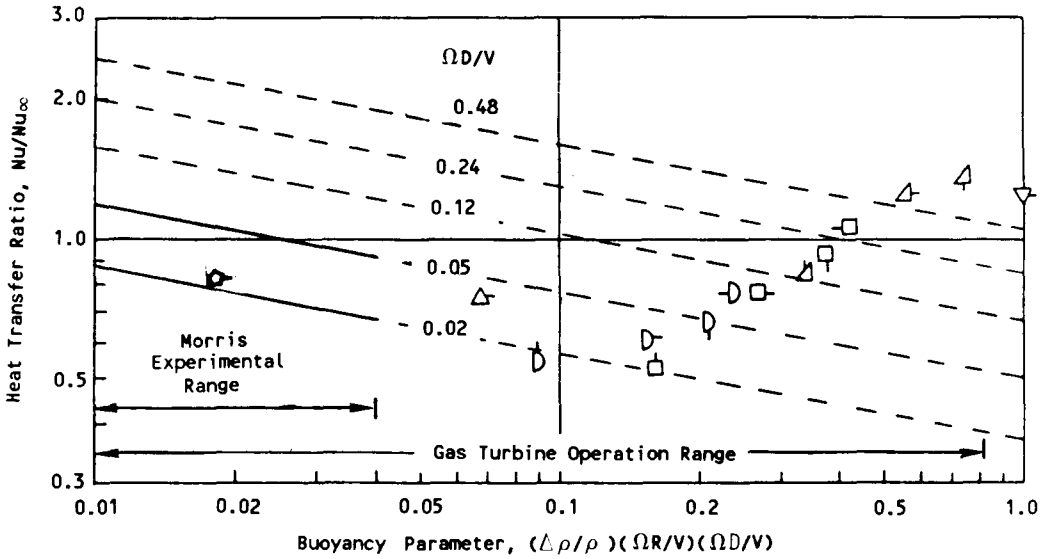

Fig. 14 Comparisons of Leading Surface Rotating Heat Transfer Results for $\overline{x}/D = 12.4$ with Morris Correlation: $Nu = 0.022\ (Ra/Re^2)^{-0.186} Ro^{0.33} Re^{0.8}$ or $Nu/Nu_\infty = 1.35\ [(\Delta\rho/\rho)*(R/D)*(\Omega D/v)^2]^{-0.186} (\Omega D/V)^{0.33}$

within Morris' experimental range which is indicated in the figure. For values of the buoyancy parameter and rotation number that fall outside the Morris data range, the present data show increases with rotation number which are in general agreement with the Morris correlation. However, the present data show increases in heat transfer with increasing density ratio or buoyancy centripetal parameter, whereas, the Morris correlation would predict a decrease in heat transfer with increasing density ratio.

The more recent results of Guidez (1988) for a smooth rectangular passage (aspect ratio 2:1) were obtained at rotation numbers up to 0.2 and values of the buoyancy parameter up to 0.1. The present results from the trailing side of the coolant passage are compatible with those of Guidez (1988) who showed heat transfer ratios of 1.7 for a Reynolds number of 24,000 and a rotation number of 0.2. However, the decrease in heat transfer ratio on the leading side of the passage shown by Guidez (i.e. $Nu/Nu_\infty = 0.7$ at $\overline{x}/D = 11.5$) was considerably less than that obtained in the present experiment (i.e. $Nu/Nu_\infty = 0.5$) for similar conditions. These differences are attributed to differences in the aspect ratios of the passages (i.e., 2:1 for Guidez's experiment compared to 1:1 for the present experiment).

CONCLUDING COMMENTS

This paper has presented an extensive body of experimental data from heat transfer experiments in a rotating square passage with smooth walls. It is believed that the large range of test parameters makes this data set unique. The extensive data base aided greatly in the data analysis and correlation and in developing physical models for the complex heat transfer characteristics.

The analysis of these experimental results to determine the separate effects of forced convection, Coriolis, and buoyancy on the heat transfer in a rotating, smooth-wall, square passage has produced the following observations and conclusions:

1. The streamwise distribution of heat transfer in the first passage from the stationary baseline experiment is similar to that from developing flow in the entrance region of a passage and is in good agreement with previous investigators' results.

2. Heat transfer is strongly affected by rotation, causing increases in heat transfer up to 3.5 times fully developed, smooth tube levels on the trailing surfaces and decreases to 40 percent of fully developed, smooth tube levels on the leading surfaces.

3. The decreases in heat transfer on the leading surfaces with increases in rotation number are attributed to the combined effects of stabilization of the near-wall flow and cross-stream flows.

4. The increases in heat transfer at the downstream locations on the leading side and the increases on the trailing side are attributed to the effects of the large scale development of Coriolis generated secondary flows.

5. Local heat transfer increases with increases in density ratio over most of the passage surface area.

6. Heat transfer decreases with increases in density ratio on the leading side of the passage near the inlet. These decreases are believed to be governed by both the interaction of the near-wall flow stability and the buoyancy effects.

7. The effects of varying Reynolds number on heat transfer ratio are reasonably well correlated by normalizing the heat transfer results with a correlation for fully developed, turbulent flow in a stationary environment.

8. Similar changes in the distributions of heat transfer occurred when either density ratio or model radius ratio were varied.

9. Increases in heat transfer ratio on the trailing surfaces were 60 percent greater than increases on the leading surfaces for the same increases in density ratio and for the same rotation number. This difference in heat transfer increase suggests that the interaction of the Coriolis and buoyancy effects is different for the flow near leading and trailing surfaces.

10. The buoyancy parameter correlates the heat transfer ratio results from the trailing side and from the most downstream location of the leading side. The results were not correlated by the buoyancy parameter near the inlet on the leading surface. The lack of correlation was attributed to a complex interaction of stabilization, buoyancy and Coriolis effects.

ACKNOWLEDGEMENTS

The work published in this paper was supported by the NASA/Lewis Research Center under the HOST Program, Contract No. NAS3-23691 to the Pratt and Whitney Commercial Engine Business/Engineering Division, and by UTC's independent research program. The heat transfer models used in this program were furnished by Pratt and Whitney. The experimental portion of the program was conducted at the United Technologies Research Center. The authors are appreciative of the support and guidance by the contract monitor team at NASA/Lewis Research Center, especially Dr. Frederick C. Yeh, and by their colleagues at P&W and UTRC.

REFERENCES

Aladyev, I. T.: Experimental Determination of Local and Mean Coefficients of Heat Transfer for Turbulent Flow in Pipes. NACA TN 1356, 1954. (Translation from Russian.)

Boelter, L. M. K., Young, G. and Iverson, H. W., NACA TN 1451, Washington, July 1948.

Brundrett, E. and Burroughs, P. R., The Temperature Inner-Law and Heat Transfer for Turbulent Air Flow in a Vertical Square Duct. Int. J. Heat Mass Transfer, Vol. 10, pp. 1133-1142, 1967.

Eckert, E. R. G., Diaguila, A. J. and Curren, A. N., Experiments on Mixed-Free- and Forced-Convective Heat Transfer Connected with Turbulent Flow Through a Short Tube. NACA Technical Note 2974, 1953.

Guidez, J., Study of the Convective Heat Transfer in Rotating Coolant Channel. ASME Paper 88-GT-33 presented in Amsterdam, The Netherlands, June, 1988.

Han, J. C., Park, J. S. and Lei, C. K, Heat Transfer and Pressure Drop in Blade Cooling Channels With Turbulence Promoters. NASA Contractor Report 3837, 1984.

Hart, J. E., Instability and Secondary Motion in a Rotating Channel Flow. J. Fluid Mech., Vol. 45, Part 2, pp. 341-351, 1971.

Iskakov, K. M. and Trushin, V. A., Influence of Rotation on Heat Transfer in a Turbine-Blade Radial Slot Channel. Izvestiya VUZ. Aviatsionnaya Tekhnika, Vol. 26, No. 1, pp. 97-99, 1983.

Johnson, B. V., Heat Transfer Experiments in Rotating Radial Passages with Supercriticl Water. ASME Heat Transfer 1978 (Bound proceedings from 1978 ASME Winter Annual Meeting).

Johnson, J. P., Halleen, R. M. and Lezius, D. K., Effects of Spanwise Rotation on the Structure of Two-Dimensional Fully Developed Turbulent Channel Flow. J. Fluid Mech., Vol . 56, Part 3, pp. 533-557, 1972.

Kays, W. M. and Perkins, H. C., Forced Convection, Internal Fow in Ducts. From Handbook of Heat Transferred Rohsenow, W. M. and Hartnett, J. P., McGraw Hill, pp. 7-28 and 7-33, Copyright 1973.

Lokai, V. I. and Gunchenko, E. I., Heat Transfer Over the Initial Section of Turbine Blade Cooling Channels Under Conditions of Rotation. Therm. Enging., Vol. 26, pp. 93-95, 1979.

Metais, B. and Eckert, E. R. G., Forced, Mixed, and Free Convection Regimes. J. Heat Transfer, Vol. 64, pp. 295-296, 1964.

Moore, J., Effects of Coriolis on Turbulent Flow in Rotating Rectangular Channels. M.I.T. Gas Turbine Laboratory Report No. 89, 1967.

Mori, Y., Fukada, T. and Nakayama, W., Convective Heat Transfer in a Rotating Radial Circular Pipe (2nd Report). Int. J. Heat Mass Transfer, Vol. 14, pp. 1807-1824, 1971.

Morris, W. D. and Ayhan, T., Observations on the Influence of Rotation on Heat Transfer in the Coolant Channels of Gas Turbine Rotor Blades. Proc. Instn. Mech. Engrs., Vol. 193, pp. 303-311, 1979.

Morris, W., Heat Transfer and Fluid Flow in Rotating Coolant Channels. Research Studies Press, Copyright 1981.

Rothe, P. H. and Johnston, J. P., Free Shear Layer Behavior in Rotating Systems. J. Fluids Enging., Vol. 101, pp. 117-120, 1979.

Sandborn, V. A., Experimental Evaluation of Momentum Terms in Turbulent Pipe Flow. NACA TN 3266, 1955.

Suo, M., Unpublished Notes, United Technologies Research Center, 1980.

Wagner, R. E. and Velkoff, H. R., Measurements of Secondary Flows in a Rotating Duct. J. Eng. for Power, ASME Paper 72-GT-17, 1972.

Yang, J. W. and Liao, N., An Experimental Study of Turbulent Heat Transfer in Converging Rectangular Ducts. Paper No. 73-WA/HT-27. ASME Journal of Heat Transfer. November 1973.